ELSEVIER

International Journal of Solids and Structures 41 (2004) 3505–3519

INTERNATIONAL JOURNAL OF SOLIDS and STRUCTURES

www.elsevier.com/locate/ijsolstr

Singular integral equation method for the solution of multiple curved crack problems

Y.Z. Chen *

Division of Engineering Mechanics, Jiangsu University, 301 Xuefu Road, Zhenjiang, Jiangsu 212013, PR China

Received 4 August 2003; received in revised form 26 January 2004
Available online 5 March 2004

Abstract

A method based on complex potentials for distributions of dislocations along curved cracks is used to solve multiple curved crack problems in plane elasticity. The method allows evaluation of the interaction between curved cracks. A crack problem is reduced to a system of singular integral equations and the crack curve length is taken as the coordinate in the associated integral equations. A crack is then mapped on the real axis in an interval $(-a, a)$, where $2a$ is the length of crack and the original singular integral equations are transformed accordingly. The method allows cracks with a general curvature and is not restricted to slightly curved crack configurations. The resulting singular integral equation system is solved through Gauss quadrature. A few numerical examples of problems with two cracks are given and crack interaction, i.e., the shielding effect of a curved crack surrounding by another, is also studied.

Keywords: Interaction of curved cracks; Numerical solution of singular integral equation

1. Introduction

The curved crack problem in plane elasticity is a special case of problems that are solvable with the boundary integral equations (BIE). The integral equations for such a problem contain a dislocation distribution or a dislocation doublet along a curved crack path and may be expressed in the general form

$$\int_L K(t,t_0)f(t)\,\mathrm{d}t = p(t_0), \quad (\text{or } p(t_0)+c,\ t_0 \in L), \tag{1}$$

where $f(t)$ is the unknown function, $K(t,t_0)$ the kernel, and $p(t_0)$ the right hand term in the equation. In Eq. (1), "L" represents the crack curve configuration. Clearly, the nature of the kernel $K(t,t_0)$ depends on the explicit choice of the functions $f(t)$ and $p(t_0)$. The possible choices of $f(t)$ and $p(t_0)$ are listed in Table 1.

In the case of WS (weakly singular) integral equations, the dislocation distribution is taken as the unknown function, and the resultant force as the right hand term (Cheung and Chen, 1987). The explicit

* Tel.: +86-5118780780; fax: +86-5118791739.
E-mail address: chens@ujs.edu.cn (Y.Z. Chen).

0020-7683/$ - see front matter © 2004 Published by Elsevier Ltd.
doi:10.1016/j.ijsolstr.2004.02.004

Table 1
Classification of the integral equations in curved crack problem

Type	$f(t)$	$p(t_0)$	Property of $K(t,t_0)$
(a) WS	Dislocations	Resultant forces	Weakly singular (log singular)
(b) S1	Dislocations	Tractions	Cauchy singular
(c) S2	Displacement jump (COD)	Resultant forces	Cauchy singular
(d) HS	Displacement jump (COD)	Tractions	Hypersingular

solution of the integral equation, whose kernel is logarithmic, is unknown, but it can however be solved numerically with the boundary element method.

In the case of S1 (Cauchy singular) integral equations, the dislocation distribution is taken as the unknown function, and the traction applied on the crack face as the right hand term. Many researchers have studied this case (Savruk, 1981; Chen et al., 1991) and some have used perturbation methods to solve the problem (Cotterell and Rice, 1980; Dreilich and Gross, 1985; Martin, 2000). In general, the range of application of previously obtained solutions for the curved crack problem is however not satisfactory. For example, in the perturbation method, a curved crack is generally projected on the real axis. Clearly, this formulation is only valid for slightly curved cracks. However, for complicated multiple crack cases, this assumption is no longer valid.

For the type S2 (Cauchy singular) integral equations, the displacement jump is the unknown function, and the resultant force on the crack face is the right hand term (Chen, 1999). There is no known explicit integration rule for the singular integral $\int_L \frac{g(t)\,dt}{t-t_0}$, where both "$t$" and "$t_0$" are located on the curve "L", and the numerical solution for a singular integral equation of this type is complicated.

For the type HS (hypersingular) integral equations, the displacement jump is taken as the unknown function and the traction on the crack face as the right hand term (Chen, 1993; Lin'kov, 1999; Mogilevskaya, 2000). Generally, the integration rule for the hypersingular integral along a curve is rather complicated.

In this paper, we will discuss the numerical solutions for the multiple curved crack problems. After placing some dislocation distributions along the curved cracks, relevant complex potentials can be formulated. In addition, the mutual influence between the curved cracks can be achieved from the obtained complex potentials. Instead of solving the original multiple curved crack problem, the governing equations are transformed to a system of the singular integral equations of the S1 type. A new method for cracks of

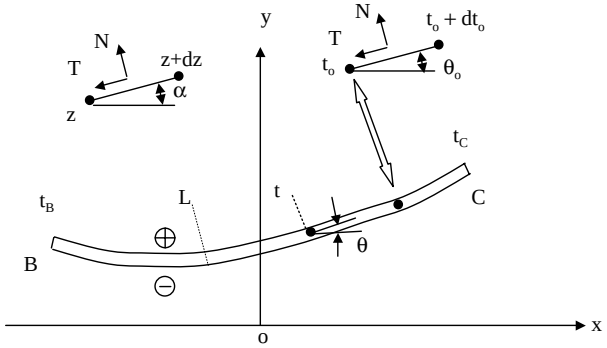

Fig. 1. The curved crack configuration and the curve length coordinate.

general curvature that is not restricted to slightly curved cracks is developed. The crack length is taken as the coordinate along the crack and the crack configuration is mapped on a real axis in an interval $(-a, a)$ (Fig. 1). The proposed method is called the 'curve length method' hereafter. A striking advantage of the method is that the integral defined on a curve can be converted to a relevant integral defined on the real axis. Therefore, known integration rules can be used for problem solution. Finally, several numerical examples are given to illustrate the efficiency of the method presented.

2. Singular integral equation for multiple curved crack problems

The fundamentals of the complex variable function method, which plays an important role in plane elasticity, are briefly introduced in what follows. In the method, the stresses $(\sigma_x, \sigma_y, \sigma_{xy})$, the resultant forces (X, Y) and the displacements (u, v) are expressed in terms of the complex potentials $\phi(z)$ and $\psi(z)$ such that (Muskhelishvili, 1953)

$$\sigma_x + \sigma_y = 4\ \mathrm{Re}\,\Phi(z),$$

$$\sigma_y - \mathrm{i}\sigma_{xy} = 2\mathrm{Re}\,\Phi(z) + z\overline{\Phi'(z)} + \overline{\Psi(z)}, \tag{2}$$

$$f = -Y + \mathrm{i}X = \phi(z) + z\overline{\phi'(z)} + \overline{\psi(z)}, \tag{3}$$

$$2G(u + \mathrm{i}v) = \kappa\phi(z) - z\overline{\phi'(z)} - \overline{\psi(z)}, \tag{4}$$

where G is the shear modulus of elasticity, $\kappa = (3 - v)/(1 + v)$ in the plane stress problem, $\kappa = 3 - 4v$ in the plane strain problem, and v is the Poisson's ratio. In Eq. (2) we denote $\Phi(z) = \phi'(z)$, $\Psi(z) = \psi'(z)$.

If the tractions applied on the curved crack are the same in magnitude and opposite in direction for the upper and lower crack faces, the complex potentials caused by a dislocation distribution $g'(t)$ along the curved crack "L" can be expressed by (Savruk, 1981; Chen, 1995)

$$\Phi(z) = \phi'(z) = \frac{1}{2\pi}\int_L \frac{g'(t)\,\mathrm{d}t}{t - z},$$

$$\Psi(z) = \psi'(z) = \frac{1}{2\pi}\int_L \frac{\overline{g'(t)}\,\mathrm{d}\bar{t}}{t - z} - \frac{1}{2\pi}\int_L \frac{\bar{t}g'(t)\,\mathrm{d}t}{(t - z)^2}, \tag{5}$$

where

$$g'(t) = -\frac{2G\mathrm{i}}{\kappa + 1}\frac{\mathrm{d}\{u(t) + \mathrm{i}v(t)\}_j}{\mathrm{d}t}, \quad (t \in L). \tag{6}$$

In Eq. (6), $(u(t) + \mathrm{i}v(t))_j (= (u(t) + \mathrm{i}v(t))^+ - (u(t) + \mathrm{i}v(t))^-)$ stands for the jump value of the displacements, and $(u(t) + \mathrm{i}v(t))^+ ((u(t) + \mathrm{i}v(t))^-)$ denotes the displacements at a point "t" of the upper (lower) face of the crack "L" (Fig. 1). The derivative $\mathrm{d}\{\}/\mathrm{d}t$ is defined (as a derivative) in a specified direction (DISD) (Chen, 1995).

Clearly, from the single-valuedness condition of displacements, the following constraint equation is obtained

$$\int_L g'(t)\,\mathrm{d}t = 0. \tag{7}$$

Two cases for the traction influence of the distributed dislocation will be investigated below. The first case is the traction influence on the crack faces themselves (Fig. 1). According to Savruk (1981) and Chen (1995), the traction on a point t_0 of crack face is

$$N(t_0)+\mathrm{i}T(t_0)=\frac{1}{\pi}\int_L\frac{g'(t)\,\mathrm{d}t}{t-t_0}+\frac{1}{2\pi}\int_L K_1(t,t_0)g'(t)\,\mathrm{d}t+\frac{1}{2\pi}\int_L K_2(t,t_0)\overline{g'(t)}\,\mathrm{d}\bar{t},\quad (t_0\in L), \tag{8}$$

where "L" denotes the curved crack configuration and

$$\begin{aligned}K_1(t,t_0)&=\frac{\mathrm{d}}{\mathrm{d}t_0}\left\{\ln\frac{t_0-t}{\bar{t}_0-\bar{t}}\right\}=-\frac{1}{t-t_0}+\frac{1}{\bar{t}-\bar{t}_0}\frac{\mathrm{d}\bar{t}_0}{\mathrm{d}t_0},\\ K_2(t,t_0)&=-\frac{\mathrm{d}}{\mathrm{d}t_0}\left\{\frac{t_0-t}{\bar{t}_0-\bar{t}}\right\}=\frac{1}{\bar{t}-\bar{t}_0}-\frac{t-t_0}{(\bar{t}-\bar{t}_0)^2}\frac{\mathrm{d}\bar{t}_0}{\mathrm{d}t_0}.\end{aligned} \tag{9}$$

In Eq. (9) the expression $\mathrm{d}\{\}/\mathrm{d}t_0$ should be defined as a DISD-derivative. Clearly, only the first integral in Eq. (8) is singular. Secondly, after assuming $\mathrm{d}t_0=\mathrm{d}s_0\exp(\mathrm{i}\theta_0)$ in Fig. 1, we have $\mathrm{d}\bar{t}_0/\mathrm{d}t_0=\exp(-2\mathrm{i}\theta_0)$. Therefore, the second and the third integrals in Eq. (8) also depend on the direction of the segment $\overline{t_0,t_0+\mathrm{d}t_0}$.

Simply by making the following substitutions: (a) $t_0\to z$, (b) $\mathrm{d}t_0\to\mathrm{d}z$ in Eqs. (8) and (9), the traction influence at a point "z" on the segment $\overline{z,z+\mathrm{d}z}$ in Fig. 1 can be expressed as

$$\begin{aligned}N(z)+\mathrm{i}T(z)=&\frac{1}{\pi}\int_L\frac{g'(t)\,\mathrm{d}t}{t-z}+\frac{1}{2\pi}\int_L K_1(t,z)g'(t)\,\mathrm{d}t+\frac{1}{2\pi}\int_L K_2(t,z)\overline{g'(t)}\,\mathrm{d}\bar{t},\\ &\text{(at a point "}z\text{" on the segment }\overline{z,z+\mathrm{d}z},\ \text{Fig. 1)},\end{aligned} \tag{10}$$

where "L" denotes the curved crack configuration and

$$\begin{aligned}K_1(t,z)&=-\frac{1}{t-z}+\frac{1}{\bar{t}-\bar{z}}\frac{\mathrm{d}\bar{z}}{\mathrm{d}z},\\ K_2(t,z)&=\frac{1}{\bar{t}-\bar{z}}-\frac{t-z}{(\bar{t}-\bar{z})^2}\frac{\mathrm{d}\bar{z}}{\mathrm{d}z}.\end{aligned} \tag{11}$$

When the integration for "t" is performed along the curve "L" in Eq. (10), the observation point "z" is different from the point "t", and thus, all integrals in Eq. (10) are regular. Note that, in Eq. (11) $\mathrm{d}\bar{z}/\mathrm{d}z(=\exp(-2\mathrm{i}\alpha))$ denotes a DISD-derivative rather than a derivative of an analytic function (Fig. 1).

For a single curved crack case, once the solution for $g'(t)$ is obtained from Eqs. (7) and (8), the stress intensity factor (SIF) at the left crack tip B in Fig. 1 can be evaluated by (Savruk, 1981; Chen, 1995)

$$(K_1-\mathrm{i}K_2)_B=\sqrt{2\pi}\operatorname*{Lim}_{t\to t_B}\sqrt{|t-t_B|}g'(t). \tag{12}$$

Similarly, for the right crack tip C we have

$$(K_1-\mathrm{i}K_2)_C=-\sqrt{2\pi}\operatorname*{Lim}_{t\to t_C}\sqrt{|t-t_C|}g'(t). \tag{13}$$

Let us consider the case of two curved cracks (Fig. 2). The problem, where tractions on the crack faces are given can be modeled by assuming a dislocation distribution $g_1'(t_1)$ along the curved crack-1 and $g_2'(t_2)$ along the curved crack-2 and using superposition. The tractions on the crack-1 are composed of two parts, which are derived from the dislocation distributions. The first part is obtained from the dislocation distribution $g_1'(t_1)$ along the curved crack-1, using Eq. (8). The second part is obtained from the dislocation distribution $g_2'(t_2)$ along the curved crack-2, using Eq. (10).

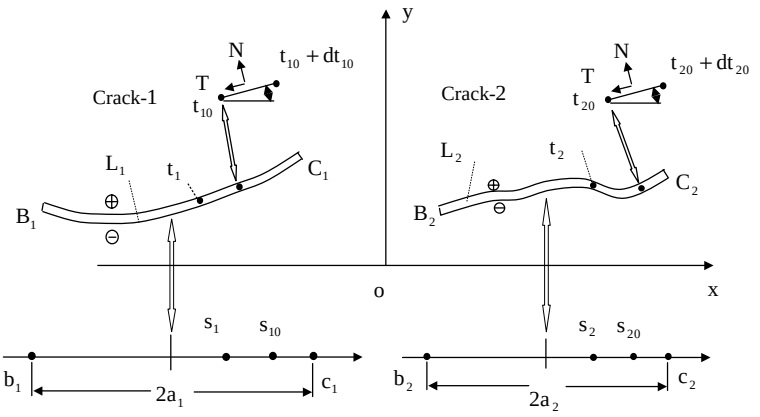

Fig. 2. Formulation of multiple curved crack problem.

Finally, superposition of the two parts results in a singular integral equation for crack-1 as follows

$$\frac{1}{\pi}\int_{L_1}\frac{g_1'(t_1)\,\mathrm{d}t_1}{t_1-t_{10}}+\frac{1}{2\pi}\int_{L_1}K_1(t_1,t_{10})g_1'(t_1)\,\mathrm{d}t_1+\frac{1}{2\pi}\int_{L_1}K_2(t_1,t_{10})\overline{g_1'(t_1)}\,\mathrm{d}\bar{t}_1+\frac{1}{\pi}\int_{L_2}\frac{g_2'(t_2)\,\mathrm{d}t_2}{t_2-t_{10}}$$
$$+\frac{1}{2\pi}\int_{L_2}K_1(t_2,t_{10})g_2'(t_2)\,\mathrm{d}t_2+\frac{1}{2\pi}\int_{L_2}K_2(t_2,t_{10})\overline{g_2'(t_2)}\,\mathrm{d}\bar{t}_2=N_1(t_{10})+\mathrm{i}T_1(t_{10})\quad(t_{10}\in L_1),\tag{14}$$

where $N_1(t_{10})+\mathrm{i}T_1(t_{10})$ denotes the tractions applied at the point t_{10} of crack-1, and

$$K_1(t_1,t_{10})=-\frac{1}{t_1-t_{10}}+\frac{1}{\bar{t}_1-\bar{t}_{10}}\frac{\mathrm{d}\bar{t}_{10}}{\mathrm{d}t_{10}},\quad K_2(t_1,t_{10})=\frac{1}{\bar{t}_1-\bar{t}_{10}}-\frac{t_1-t_{10}}{(\bar{t}_1-\bar{t}_{10})^2}\frac{\mathrm{d}\bar{t}_{10}}{\mathrm{d}t_{10}},\tag{15}$$

$$K_1(t_2,t_{10})=-\frac{1}{t_2-t_{10}}+\frac{1}{\bar{t}_2-\bar{t}_{10}}\frac{\mathrm{d}\bar{t}_{10}}{\mathrm{d}t_{10}},\quad K_2(t_2,t_{10})=\frac{1}{\bar{t}_2-\bar{t}_{10}}-\frac{t_2-t_{10}}{(\bar{t}_2-\bar{t}_{10})^2}\frac{\mathrm{d}\bar{t}_{10}}{\mathrm{d}t_{10}}.\tag{16}$$

Note that, the first three integrals in Eq. (14) represent the influence on the crack-1 caused by the dislocations on the crack itself, and the second three integrals in Eq. (14) represent the influence from the dislocations on crack-2. Note that, except for the first integral in Eq. (14), all integrals in Eq. (14) are regular. In addition, the single-valuedness condition for crack-1 will lead to

$$\int_{L_1}g'(t_1)\,\mathrm{d}t_1=0.\tag{17}$$

Similarly, a singular integral equation can be formulated for the crack-2 in Fig. 2

$$\frac{1}{\pi}\int_{L_2}\frac{g_2'(t_2)\,\mathrm{d}t_2}{t_2-t_{20}}+\frac{1}{2\pi}\int_{L_2}K_1(t_2,t_{20})g_2'(t_2)\,\mathrm{d}t_2+\frac{1}{2\pi}\int_{L_2}K_2(t_2,t_{20})\overline{g_2'(t_2)}\,\mathrm{d}\bar{t}_2+\frac{1}{\pi}\int_{L_1}\frac{g_1'(t_1)\,\mathrm{d}t_1}{t_1-t_{20}}$$
$$+\frac{1}{2\pi}\int_{L_1}K_1(t_1,t_{20})g_1'(t_1)\,\mathrm{d}t_1+\frac{1}{2\pi}\int_{L_1}K_2(t_1,t_{20})\overline{g_1'(t_1)}\,\mathrm{d}\bar{t}_1=N_2(t_{20})+\mathrm{i}T_2(t_{20}),\quad(t_{20}\in L_2),\tag{18}$$

where $N_2(t_{20})+\mathrm{i}T_2(t_{20})$ denotes the tractions applied at the point t_{20} of crack-2, and

$$K_1(t_2,t_{20})=-\frac{1}{t_2-t_{20}}+\frac{1}{\bar{t}_2-\bar{t}_{20}}\frac{\mathrm{d}\bar{t}_{20}}{\mathrm{d}t_{20}},\quad K_2(t_2,t_{20})=\frac{1}{\bar{t}_2-\bar{t}_{20}}-\frac{t_2-t_{20}}{(\bar{t}_2-\bar{t}_{20})^2}\frac{\mathrm{d}\bar{t}_{20}}{\mathrm{d}t_{20}},\tag{19}$$

$$K_1(t_1,t_{20}) = -\frac{1}{t_1 - t_{20}} + \frac{1}{\bar{t}_1 - \bar{t}_{20}}\frac{\mathrm{d}\bar{t}_{20}}{\mathrm{d}t_{20}}, \quad K_2(t_1,t_{20}) = \frac{1}{\bar{t}_1 - \bar{t}_{20}} - \frac{t_1 - t_{20}}{(\bar{t}_1 - \bar{t}_{20})^2}\frac{\mathrm{d}\bar{t}_{20}}{\mathrm{d}t_{20}}. \tag{20}$$

As before, the relevant constraint equation is as follows

$$\int_{L_2} g'(t_2)\,\mathrm{d}t_2 = 0. \tag{21}$$

In the case of two curved cracks, the first step is to obtain the solution for $g_1'(t_1)$ and $g_2'(t_2)$ from Eqs. (14), (17), (18) and (21).

The curve length method is used to solve the integral equations numerically and the configuration of crack-1 is mapped on the real axis "s_1" with a crack length "$2a_1$" (Fig. 2). Clearly, this is a one-to-one mapping, i.e., for a point "t_1" on the curved crack, there is a mapping point "s_1" on the real axis, and the inverse is also true.

The mapping is expressed by the function $t_1(s_1)$. After mapping, the function $g_1'(t_1)$ is rewritten in the form

$$g_1'(t_1) = h_1(s_1) = \frac{H_1(s_1)}{\sqrt{a_1^2 - s_1^2}}, \quad (\text{where } H_1(s_1) = H_{1\mathrm{r}}(s_1) + \mathrm{i}H_{1\mathrm{i}}(s_1)). \tag{22}$$

In Eq. (22), the assumed expression $h_1(s_1) = H_1(s_1)/\sqrt{a_1^2 - s_1^2}$ is obtained from the behavior of the dislocation distribution in the vicinity of a crack tip.

Similar, after using the substitution $t_2(s_2)$, the function $g_2'(t_2)$ can be rewritten as

$$g_2'(t_2) = h_2(s_2) = \frac{H_2(s_2)}{\sqrt{a_2^2 - s_2^2}}, \quad (\text{where } H_2(s_2) = H_{2\mathrm{r}}(s_2) + \mathrm{i}H_{2\mathrm{i}}(s_2)). \tag{23}$$

In the curve length method, all integrals in Eqs. (14), (17), (18) and (21) can be transformed to integrals on the real axis. It is sufficient to describe three of them as follows. The first integral in Eq. (14) may be rewritten in the form

$$I_1 = \frac{1}{\pi}\int_{L_1} \frac{g_1'(t_1)\,\mathrm{d}t_1}{t_1 - t_{10}} = \frac{1}{\pi}\int_{-a_1}^{a_1} \frac{H_1(s_1)}{\sqrt{a_1^2 - s_1^2}}\frac{A(s_1,s_{10})}{s_1 - s_{10}}\,\mathrm{d}s_1, \tag{24}$$

where

$$A(s_1,s_{10}) = \frac{(s_1 - s_{10})\mathrm{d}t_1}{(t_1 - t_{10})\mathrm{d}s_1}. \tag{25}$$

The second integral in Eq. (14) can be written as

$$I_2 = \frac{1}{2\pi}\int_{L_1} K_1(t_1,t_{10})g_1'(t_1)\,\mathrm{d}t_1 = \frac{1}{2\pi}\int_{-a_1}^{a_1} \frac{H_1(s_1)}{\sqrt{a_1^2 - s_1^2}}B(s_1,s_{10})\,\mathrm{d}s_1, \tag{26}$$

where

$$B(s_1,s_{10}) = K_1(t_1,t_{10})\frac{\mathrm{d}t_1}{\mathrm{d}s_1}. \tag{27}$$

Thirdly, the integral in Eq. (17) can be expressed by

$$I_3 = \int_{L_1} g_1'(t_1)\,\mathrm{d}t_1 = \int_{-a_1}^{a_1} \frac{H_1(s_1)}{\sqrt{a_1^2 - s_1^2}}C(s_1)\,\mathrm{d}s_1, \tag{28}$$

where

$$C(s_1) = \frac{\mathrm{d}t_1}{\mathrm{d}s_1}. \tag{29}$$

For numerical solution of the integral equation, the following Gauss integration rules for a regular function $H(s)$ are introduced (Erdogan et al., 1973; Savruk, 1981)

$$\frac{1}{\pi}\int_{-a}^{a}\frac{H(s)\,\mathrm{d}s}{\sqrt{a^2-s^2}(s-s_{0,m})} = \frac{1}{M}\sum_{j=1}^{M}\frac{H(s_j)}{s_j - s_{0,m}}, \tag{30}$$

$$\frac{1}{\pi}\int_{-a}^{a}\frac{H(s)\,\mathrm{d}s}{\sqrt{a^2-s^2}} = \frac{1}{M}\sum_{j=1}^{M}H(s_j), \tag{31}$$

where M is some integer, and

$$s_j = a\cos\frac{(j-0.5)\pi}{M} \quad (j = 1,2,\ldots,M), \tag{32}$$

$$s_{0,m} = a\cos\frac{m\pi}{M} \quad (m = 1,2,\ldots,M-1). \tag{33}$$

Note that, the integration rule (30) is only valid for the particular points $s_{0,m} = a\cos(m\pi/M)$ $(m = 1,2,\ldots,M-1)$.

If the $H(s_j)$ $(j = 1,2,\ldots,M)$ values are known beforehand, the $H(-a)$ and $H(a)$ values can be obtained from the following extrapolation formulae (Savruk, 1981)

$$\begin{aligned} H(-a) &= \frac{1}{M}\sum_{j=1}^{M}(-1)^{j+M}H(s_j)\tan((2j-1)\pi/4M),\\ H(a) &= \frac{1}{M}\sum_{j=1}^{M}(-1)^{j+1}H(s_j)\cot((2j-1)\pi/4M). \end{aligned} \tag{34}$$

The numerical solution for the multiple curved crack problems is composed of the following steps.

(a) Depending on the crack lengths, M_1 is assumed for the number of abscissas for crack-1. Similarly, M_2 is assumed for crack-2.
(b) After substituting Eqs. (22) and (23) into Eqs. (14), (17), (18) and (21), and using the integration rules (30) and (31), the latter can be reduced to a system of algebraic equations with respect to the following unknowns

$$\begin{aligned} &\mathrm{Re}\{H_1(s_{1,m})\}\mathrm{Im}\{H_1(s_{1,m})\} \quad \text{with } s_{1,m} = a_1\cos\frac{(m-0.5)\pi}{M_1} \quad (m = 1,2,\ldots,M_1),\\ &\mathrm{Re}\{H_2(s_{2,m})\}\mathrm{Im}\{H_2(s_{2,m})\} \quad \text{with } s_{2,m} = a_2\cos\frac{(m-0.5)\pi}{M_2} \quad (m = 1,2,\ldots,M_2). \end{aligned} \tag{35}$$

Furthermore, a solution for $H_1(s_{1,m})$ $(m = 1,2,\ldots,M_1)$ and $H_2(s_{2,m})$ $(m = 1,2,\ldots,M_2)$ is obtainable.
(c) From the obtained $H_1(s_{1,m})$ and $H_2(s_{2,m})$, the extrapolation formulae Eq. (34) yield $H_1(-a_1)$, $H_1(a_1)$, $H_2(-a_2)$ and $H_2(a_2)$.
(d) From Eqs. (12) and (13), the stress intensity factor (SIF) at the crack tips B_1 and C_1 of crack-1 in Fig. 2 can be evaluated by

$$(K_1 - \mathrm{i}K_2)_{B_1} = \sqrt{\frac{\pi}{a_1}}H_1(-a_1), \quad (K_1 - \mathrm{i}K_2)_{C_1} = -\sqrt{\frac{\pi}{a_1}}H_1(a_1). \tag{36}$$

Similarly, the stress intensity factor (SIF) at the crack tips B_2 and C_2 of crack-2 in Fig. 2 can be evaluated by

$$(K_1 - \mathrm{i}K_2)_{B_2} = \sqrt{\frac{\pi}{a_2}} H_2(-a_2), \quad (K_1 - \mathrm{i}K_2)_{C_2} = -\sqrt{\frac{\pi}{a_2}} H_2(a_2). \tag{37}$$

For the circular arc crack case, for example, under the action of remote the stress σ_{xy}^{∞} the COD (crack opening displacement) may be negative for certain values, indicating overlapping of the crack faces. Naturally, in this case, compatibility is violated. In this paper, a non-overlapping condition in terms of COD is introduced. For a curved crack case, once the function $g'(t)$ is obtained from the numerical solution, the COD function at a point "t", Fig. 1, can be obtained from Eq. (6)

$$u(t) + \mathrm{i}v(t) = -\frac{(\kappa + 1)}{2Gi} \int_{t_B}^{t} g'(t)\,\mathrm{d}t. \tag{38}$$

Note that in Eq. (38) the subscript "j" has been omitted for the sake of simplification. A further expression for COD is introduced

$$u_1(t) + \mathrm{i}v_1(t) = (u(t) + \mathrm{i}v(t))\mathrm{e}^{-\mathrm{i}\theta(t)}, \tag{39}$$

where $\theta(t)$ denotes the tangent angle at the point "t" (Fig. 1). Clearly, the non-overlapping condition for COD can be expressed as

$$v_1(t) \geqslant 0. \tag{40}$$

This condition is checked in the numerical examples.

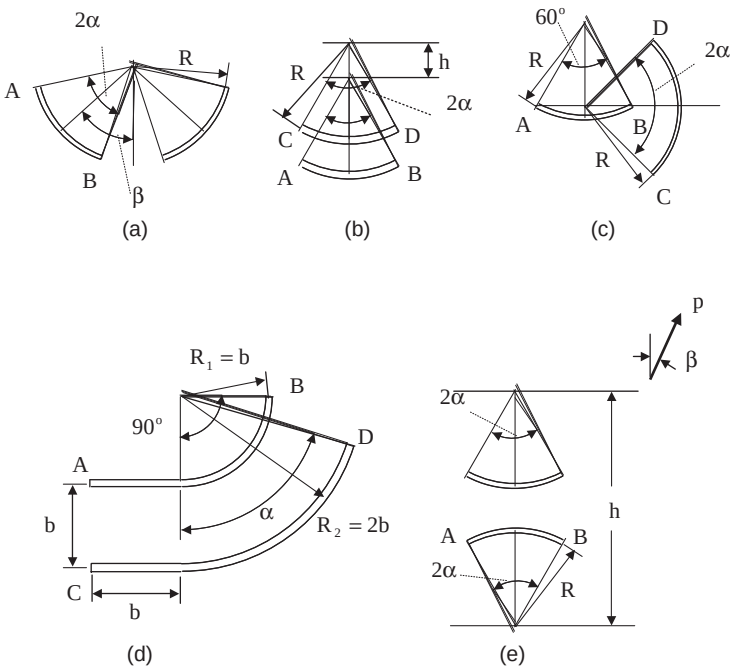

Fig. 3. Five cases of multiple curved crack: (a) two circular arc cracks on the same circle, (b) two circular arc cracks in a stacked position, (c) two circular arc cracks in a complicated position, (d) two line-circular arc cracks, (e) two circular arc cracks with an inclined remote tension.

Before studying the numerical examples, a known result is used. For a single circular arc crack with the remote traction case of σ_x^∞, σ_y^∞ and σ_{xy}^∞, the SIFs at the crack tips "A" and "B" in Fig. 3(e) can be expressed by (Cotterell and Rice, 1980)

$$K_{1A} = f_{1A}\sqrt{\pi R \sin\alpha}, \quad K_{1B} = f_{1B}\sqrt{\pi R \sin\alpha}, \tag{41}$$

$$K_{2A} = f_{2A}\sqrt{\pi R \sin\alpha}, \quad K_{2B} = f_{2B}\sqrt{\pi R \sin\alpha}, \tag{42}$$

where

$$\begin{aligned} \begin{matrix} f_{1A} \\ f_{1B} \end{matrix} &= \left\{ \left(\frac{\sigma_y^\infty + \sigma_x^\infty}{2} \right) - \left(\frac{\sigma_y^\infty - \sigma_x^\infty}{2} \right) \sin^2(\alpha/2)\cos^2(\alpha/2) \right\} \frac{\cos(\alpha/2)}{1+\sin^2(\alpha/2)} \\ &\quad + \left\{ \frac{\sigma_y^\infty - \sigma_x^\infty}{2} \right\} \cos(3\alpha/2) \mp \sigma_{xy}^\infty \{ \sin(3\alpha/2) + \sin^3(\alpha/2) \}, \end{aligned} \tag{43}$$

$$\begin{aligned} \begin{matrix} f_{2A} \\ f_{2B} \end{matrix} &= \pm \left\{ \left(\frac{\sigma_y^\infty + \sigma_x^\infty}{2} \right) - \left(\frac{\sigma_y^\infty - \sigma_x^\infty}{2} \right) \sin^2(\alpha/2)\cos^2(\alpha/2) \right\} \frac{\sin(\alpha/2)}{1+\sin^2(\alpha/2)} \\ &\quad \pm \left\{ \frac{\sigma_y^\infty - \sigma_x^\infty}{2} \right\} \sin(3\alpha/2) + \sigma_{xy}^\infty \{ \cos(3\alpha/2) + \cos(\alpha/2)\sin^2(\alpha/2) \}. \end{aligned} \tag{44}$$

3. Numerical examples

Some numerical examples are given to illustrate the results of the method presented.

Example 1. In the first example, two circular arc cracks on the same circle are subjected to the remote tension $\sigma_x^\infty = \sigma_y^\infty = p$ (Fig. 3(a)). In the computation, $M_1 = M_2 = 45$ in Eq. (35) is used. The calculated results for the SIFs at the crack tips "A" and "B" are expressed as

$$\begin{aligned} &K_{1A} = F_{1A}(\alpha/\beta,\beta)p\sqrt{\pi R \sin\alpha}, \quad K_{2A} = F_{2A}(\alpha/\beta,\beta)p\sqrt{\pi R \sin\alpha}, \\ &K_{1B} = F_{1B}(\alpha/\beta,\beta)p\sqrt{\pi R \sin\alpha}, \quad K_{2B} = F_{2B}(\alpha/\beta,\beta)p\sqrt{\pi R \sin\alpha} \end{aligned} \tag{45}$$

and are plotted in Figs. 4 and 5. The results show that the stress intensity factor at the inner crack tip "B" is generally higher than at the outer crack tip "A". For example, in the case of $\beta = 30^\circ$ and $\alpha/\beta = 0.9$, the results $F_{1A} = 0.8919$ and $F_{1B} = 1.2424$ is obtained.

Example 2. In the second example, two stacked circular cracks are subjected to the remote tension $\sigma_x^\infty = \sigma_y^\infty = p$ (Fig. 3(b)). In the computation, $M_1 = M_2 = 75$ in Eq. (35) is used. The calculated results for the SIFs at the crack tips "B" and "D" are expressed as

$$\begin{aligned} &K_{1B} = F_{1B}(h/2R,\alpha)p\sqrt{\pi R \sin\alpha}, \quad K_{2B} = F_{2B}(h/2R,\alpha)p\sqrt{\pi R \sin\alpha}, \\ &K_{1D} = F_{1D}(h/2R,\alpha)p\sqrt{\pi R \sin\alpha}, \quad K_{2D} = F_{2D}(h/2R,\alpha)p\sqrt{\pi R \sin\alpha} \end{aligned} \tag{46}$$

and are plotted in Fig. 6. Since there is no symmetry in the y-direction, the severity at the crack tip "D" is different from that at the tip "B". For example, in the case of $\alpha = \pi/2$ and $h/2R = 0.2$, we have $F_{1D} = 0.5728$, $F_{2D} = 0.4409$ and $F_{1B} = 0.1463$, $F_{2B} = 0.0685$. That is to say, crack extension is generally initiated at the crack tip "D". If the distance between the two cracks is increased, the difference between the

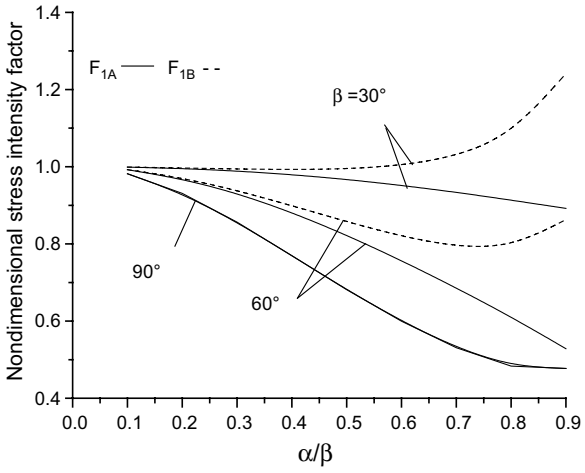

Fig. 4. Non-dimensional SIFs $F_{1A}(\alpha/\beta,\beta)$ and $F_{1B}(\alpha/\beta,\beta)$ for the multiple curved cracks (see Fig. 3(a) and Eq. (45)).

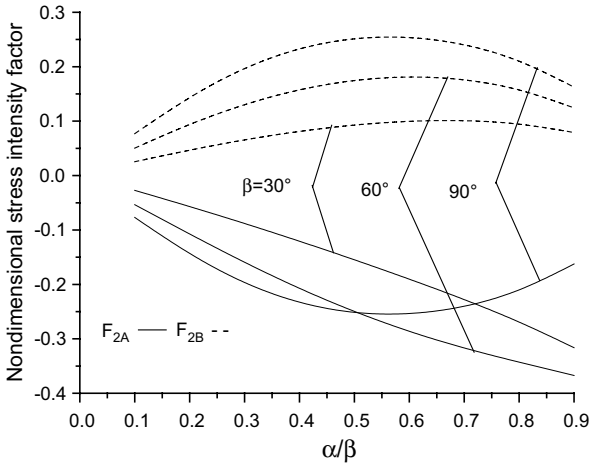

Fig. 5. Non-dimensional SIFs $F_{2A}(\alpha/\beta,\beta)$ $K_{2B}=F_{2B}(\alpha/\beta,\beta)$ for the multiple curved cracks (see Fig. 3(a) and Eq. (45)).

stress intensity factors at the crack tips "D" and "B", respectively, is smaller. For example, in the case of $\alpha=\pi/2$ and $h/2R=1.0$, we have $F_{1D}=0.5653$, $F_{2D}=0.4319$ and $F_{1B}=0.5377$, $F_{2B}=0.3631$.

Example 3. In the third example, two circular arc cracks are subjected to the remote tension $\sigma_x^\infty=\sigma_y^\infty=p$ (Fig. 3(c)). The spanning angle of the first crack is $\pi/3$, and of the second is 2α. In the computation, we take $M_1=35$, $M_2=M_1*\sqrt{a_2/a_1}$, where a_1 (a_2) is the half-length of the first (second) crack. The calculated results for the SIFs at the crack tips "A", "B", "C" and "D" are expressed as

$$\begin{aligned}
&K_{1A}=F_{1A}(\alpha)p\sqrt{\pi R\sin(\pi/6)}, \quad K_{2A}=F_{2A}(\alpha)p\sqrt{\pi R\sin(\pi/6)},\\
&K_{1B}=F_{1B}(\alpha)p\sqrt{\pi R\sin(\pi/6)}, \quad K_{2B}=F_{2B}(\alpha)p\sqrt{\pi R\sin(\pi/6)},\\
&K_{1C}=F_{1C}(\alpha)p\sqrt{\pi R\sin\alpha}, \quad K_{2C}=F_{2C}(\alpha)p\sqrt{\pi R\sin\alpha},\\
&K_{1D}=F_{1D}(\alpha)p\sqrt{\pi R\sin\alpha}, \quad K_{2D}=F_{2D}(\alpha)p\sqrt{\pi R\sin\alpha}
\end{aligned} \tag{47}$$

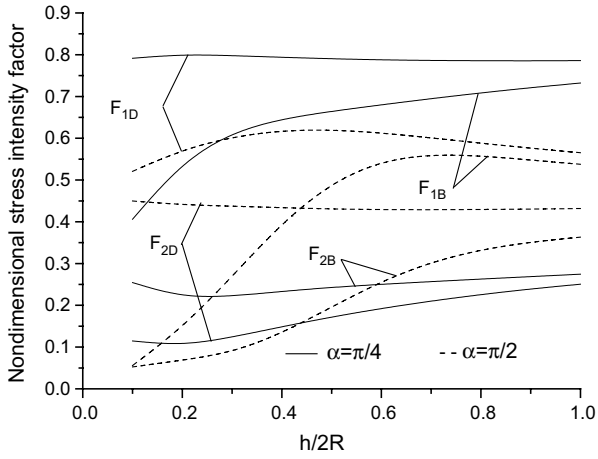

Fig. 6. Non-dimensional SIFs $F_{1B}(h/2R,\alpha)$, $F_{2B}(h/2R,\alpha)$, $F_{1D}(h/2R,\alpha)$ and $F_{2D}(h/2R,\alpha)$ for the multiple curved cracks (see Fig. 3(b) and Eq. (46)).

and the results are plotted in Fig. 7. Since the spanning angle of the second crack (2α) is varied, the shielding effect for the first crack is easily seen. For example, in the case of $\alpha = \pi/18$ ($=10°$), we have $F_{1A} = 0.9078$, $F_{2A} = -0.2518$, $F_{1B} = 0.9145$ and $F_{2B} = 0.2692$. However, in the case of $\alpha = 7\pi/18$ ($=70°$), we have $F_{1A} = 0.7470$, $F_{2A} = -0.4642$, $F_{1B} = 0.1248$ and $F_{2B} = 0.1935$. For the two cases, the reduction factor for F_{1B} is 0.1365 ($=0.1248/0.9145$). The result shows that as a smaller curved crack is surrounded by a larger curved crack, the severity at the crack tips of the smaller crack is not significant.

Example 4. In the fourth example, two line-circular arc cracks are subjected to the remote tension $\sigma_x^\infty = \sigma_y^\infty = p$ (Fig. 3(d)). The geometry of the first crack is kept constant, and the spanning angle α of the second crack changes from $15°, 30°, \ldots, 180°$. In the computation, we take $M_1 = 35$, $M_2 = M_1 * \sqrt{a_2/a_1}$, where a_1 (a_2) is the half-length of the first (second) crack. The calculated results for the SIFs at the crack tips "A","B", "C" and "D" are expressed as

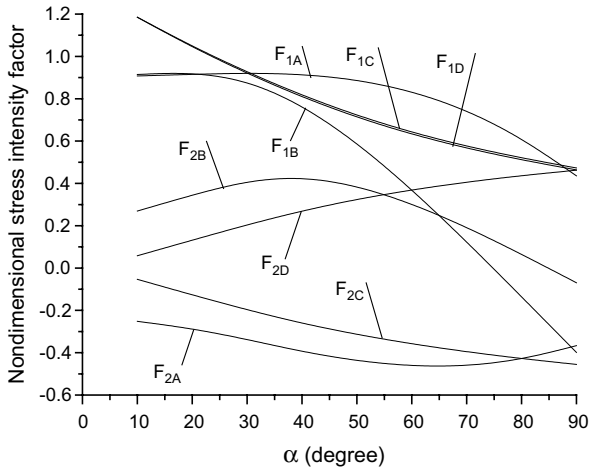

Fig. 7. Non-dimensional SIFs $F_{1A}(\alpha)$, $F_{2A}(\alpha)$, $F_{1B}(\alpha)$, $F_{2B}(\alpha)$, $F_{1C}(\alpha)$, $F_{2C}(\alpha)$, $F_{1D}(\alpha)$ and $F_{2D}(\alpha)$ for the multiple curved cracks (see Fig. 3(c) and Eq. (47)).

$$\begin{aligned} K_{1A} &= F_{1A}(\alpha)p\sqrt{\pi b}, \quad K_{2A} = F_{2A}(\alpha)p\sqrt{\pi b}, \\ K_{1B} &= F_{1B}(\alpha)p\sqrt{\pi b}, \quad K_{2B} = F_{2B}(\alpha)p\sqrt{\pi b}, \\ K_{1C} &= F_{1C}(\alpha)p\sqrt{\pi b}, \quad K_{2C} = F_{2C}(\alpha)p\sqrt{\pi b}, \\ K_{1D} &= F_{1D}(\alpha)p\sqrt{\pi b}, \quad K_{2D} = F_{2D}(\alpha)p\sqrt{\pi b} \end{aligned} \tag{48}$$

and the results are plotted in Fig. 8. Since the spanning angle of the second crack (α) is varied, the shielding effect for the first crack is easily seen. However, the F_{1B} value is negative for a spanning angle greater than approximately $\alpha = 6\pi/12\ (=90°)$ and the solution is thus no longer valid in this case. For positive SIFs, it is seen that the shielding effect at the crack tip "A" is much weaker than that at the crack tip "B".

Example 5. In the example, we assume that the spanning angle of the arcs is $2\alpha = \pi/2\ (=90°)$ (Fig. 3(e)) the distance between the two arc centers is denoted by "h", and $M_1 = M_2 = 75$ is taken. Two loading cases: (a) $\sigma_x^\infty = \sigma_y^\infty = p$, (b) $\sigma_y^\infty = p$ are considered. For both cases the calculated SIFs at the crack tip "A " are expressed by

$$K_{1A} = F_{1A}(h/2R)p\sqrt{\pi R\sin\alpha}, \quad K_{2A} = F_{2A}(h/2R)p\sqrt{\pi R\sin\alpha}. \tag{49}$$

The calculated results of $F_{1A}(h/2R)$ and $F_{2A}(h/2R)$ for $h/2R = 1.5, 2.0, \ldots, 5.5, 10^4$ are listed in Table 2. The last term marked with "$*$" in Table 2 is obtained from Eqs. (43) and (44). As expected, when $h/2R \to \infty$, the calculated results should approach the single circular arc crack case. This agreement is confirmed by the tabulated results.

With $h/2R = 1.5$, $2\alpha = \pi/2$ and $\sigma_y^\infty = p$, for the lower crack in Fig. 3(e) the calculated COD functions shown by Eq. (39) can be expressed as

$$u_1 = \frac{(\kappa+1)p}{2G}u_1*(s/a), \quad v_1 = \frac{(\kappa+1)p}{2G}v_{1^*}(s/a) \quad |s| < a \ (\text{with } a = R\alpha), \tag{50}$$

where "s" is the coordinate of the point "t" in the curve length coordinate. The results (Fig. 9) shows that the non-overlapping condition Eq. (40), is satisfied in present case.

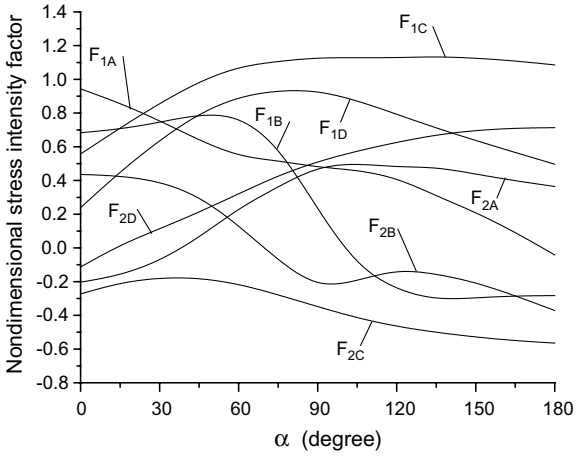

Fig. 8. Non-dimensional SIFs $F_{1A}(\alpha)$, $F_{2A}(\alpha)$, $F_{1B}(\alpha)$, $F_{2B}(\alpha)$, $F_{1C}(\alpha)$, $F_{2C}(\alpha)$, $F_{1D}(\alpha)$ and $F_{2D}(\alpha)$ for the multiple curved cracks (see Fig. 3(d) and Eq. (48)).

Table 2
Non-dimensional SIFs $F_{1A}(h/2R)$ and $F_{2A}(h/2R)$ for two circular arc cracks in a stacked position (see Fig. 3(e) and Eq. (49))

$\sigma_x^\infty = \sigma_y^\infty = p$, $2\alpha = \pi/2$ *case*											
$h/2R$	1.5	2.0	2.5	3.0	3.5	4.0	4.5	5.0	5.5	10^4	*
F_{1A}	0.7876	0.7890	0.7933	0.7967	0.7990	0.8006	0.8017	0.8026	0.8032	0.8060	0.8059
F_{2A}	0.2294	0.2763	0.2997	0.3117	0.3185	0.3227	0.3254	0.3272	0.3285	0.3339	0.3338
$\sigma_y^\infty = p$, $2\alpha = \pi/2$ *case*											
$h/2R$	1.5	2.0	2.5	3.0	3.5	4.0	4.5	5.0	5.5	10^4	*
F_{1A}	0.5225	0.5247	0.5298	0.5337	0.5364	0.5381	0.5394	0.5403	0. 5410	0.5440	0.5439
F_{2A}	0.4987	0.5467	0.5717	0.5847	0.5919	0.5963	0.5992	0.6011	0. 6025	0.6081	0.6080

* From an exact solution for a single circular arc crack, shown by Eqs. (43) and (44).

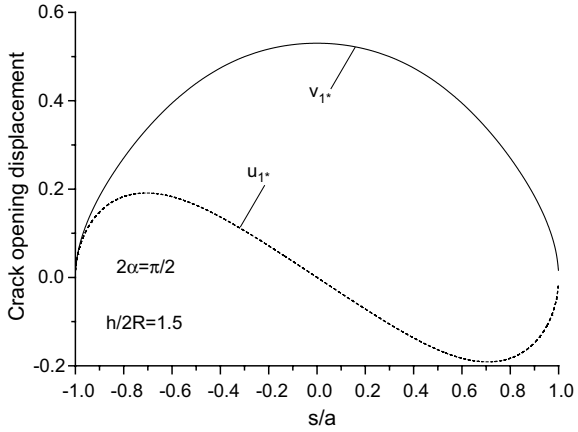

Fig. 9. Calculated results for CODs (u_{1*}, v_{1*}) in case of $h/2R = 1.5$, $2\alpha = \pi/2$ and $\sigma_y^\infty = p$ (see Fig. 3(e) and and Eq. (50)).

Table 3
Non-dimensional SIFs $F_{1A}(h/2R)$, $F_{1B}(h/2R)$, $F_{2A}(h/2R)$ and $F_{2B}(h/2R)$ for two circular arc cracks in a stacked position with an inclined tension "p" (see Fig. 3(e) and Eqs. (51) and (52))

$2\alpha = \pi/3$, $\beta = \pi/12$											
$h/2R$	1.5	2.0	2.5	3.0	3.5	4.0	4.5	5.0	5.5	10^4	*
F_{1A}	0.4709	0.5140	0.5315	0.5397	0.5441	0.5466	0.5482	0.5493	0.5501	0.5532	0.5532
F_{1B}	0.8791	0.8910	0.9005	0.9057	0.9087	0.9105	0.9116	0.9124	0.9130	0.9154	0.9154
F_{2A}	0.5265	0.5797	0.5970	0.6040	0.6075	0.6094	0.6106	0.6113	0.6119	0.6138	0.6139
F_{2B}	−0.1413	−0.1894	−0.2079	−0.2159	−0.2200	−0.2224	−0.2238	−0.2248	−0.2254	−0.2280	−0.2280
$2\alpha = \pi/3$, $\beta = 3\pi/12$											
$h/2R$	1.5	2.0	2.5	3.0	3.5	4.0	4.5	5.0	5.5	10^4	*
F_{1A}	0.0138	0.0591	0.0741	0.0806	0.0839	0.0858	0.0870	0.0877	0.0883	0.0904	0.0904
F_{1B}	0.8302	0.8133	0.8122	0.8126	0.8131	0.8135	0.8137	0.8139	0.8141	0.8148	0.8149
F_{2A}	0.4617	0.4928	0.5007	0.5036	0.5050	0.5057	0.5061	0.5064	0.5065	0.5072	0.5072
F_{2B}	0.3087	0.2879	0.2774	0.2725	0.2699	0.2684	0.2674	0.2668	0.2663	0.2646	0.2646

* From an exact solution for a single circular arc crack, shown by Eqs. (43) and (44).

Example 6. In the example, we assume that the spanning angle of the arcs is $2\alpha = \pi/3$ ($= 60°$) (Fig. 3(e)) the distance between two arc centers is denoted by "h", and $M_1 = M_2 = 75$ is taken. The remote loading "p" is

inclined an angle "β" with respect to the vertical direction. In this case, the calculated SIFs at the crack tip "A" and "B" are expressed by

$$K_{1A} = F_{1A}(h/2R)p\sqrt{\pi R\sin\alpha}, \quad K_{2A} = F_{2A}(h/2R)p\sqrt{\pi R\sin\alpha}, \tag{51}$$

$$K_{1B} = F_{1B}(h/2R)p\sqrt{\pi R\sin\alpha}, \quad K_{2B} = F_{2B}(h/2R)p\sqrt{\pi R\sin\alpha} \tag{52}$$

and the results of $F_{1A}(h/2R)$, $F_{1B}(h/2R)$, $F_{2A}(h/2R)$ and $F_{2B}(h/2R)$ for $h/2R = 1.5, 2.0, \ldots, 5.5, 10^4$ are listed in Table 3. The last term marked with "$*$" in Table 3 is obtained from a substitution of $\sigma_x^\infty = p\sin^2\beta$, $\sigma_y^\infty = p\cos^2\beta$, $\sigma_{xy}^\infty = p\sin\beta\cos\beta$ into Eqs. (43) and (44). Clearly, when $h/2R \to \infty$, the calculated results should approach the single circular arc crack case. As before, this agreement is confirmed from the tabulated results.

4. Conclusions

Since no integration rule was suggested to evaluate a singular integral along the curve, previously one had to use the boundary element method to solve the curved crack problem. In this case, some computation error may exist when discretization is performed along the curve configuration. Meantime, the discretization is generally a complicated work in computation. In the present study, we avoid using the discretization and the curve length method is introduced. Many integration rules used on a real axis can be used to the multiple curved crack problems. This will considerably reduce effort to get the final numerical results.

In this paper, the mapping relation for crack-1 is expressed by the function $t_1(s_1)$. In computation, one should find the following items: (a) the length a_1, (b) the mapping relation $t_{1,m}$ and $s_{1,m} = a_1\cos((m-0.5)\pi/M_1)$, $(m = 1, 2, \ldots, M_1)$. In fact, for any complicated geometry of crack, the length a_1 can be evaluated by a numerical integration. Secondly, the relation between $t_{1,m}$ and $s_{1,m}$ can easily be found by using a numerical iteration procedure. From the knowledge of author, the mentioned computation can be performed on computer without any difficulty.

Acknowledgements

The project was supported by National Natural Science Foundation of China. The author is grateful to referees for proposing many comments and for polishing the manuscript throughout.

References

Chen, Y.Z., 1993. Numerical solution of a curved crack problem by using hypersingular integral equation. Eng. Fract. Mech. 46, 275–283.

Chen, Y.Z., 1995. A survey of new integral equation in plane elasticity crack problem. Eng. Fract. Mech. 51, 97–134.

Chen, Y.Z., 1999. Stress intensity factors for curved and kinked cracks in plane extension. Theo. Appl. Fract. Mech. 31, 223–232.

Chen, Y.Z., Gross, D., Huang, Y.J., 1991. Numerical solution of the curved crack problem by means of polynomial approximation of the dislocation distribution. Eng. Fract. Mech. 39, 791–797.

Cheung, Y.K., Chen, Y.Z., 1987. New integral equation for plane elasticity crack problem. Theo. Appl. Fract. Mech. 7, 177–184.

Cotterell, B., Rice, J.R., 1980. Slightly curved or kinked cracks. Int. J. Fract 16, 155–169.

Dreilich, L., Gross, D., 1985. The curved crack. Z. Angew. Math. Mech. 65, 132–134.

Erdogan, F., Gupta, G.D., Cook, T.S., 1973. Numerical solution of singular integral equation. In: Sih, G.C. (Ed.), Mechanics of Fracture, vol. 1. Noordhoff, Netherlands, pp. 368–425.

Lin'kov, A.M., 1999. Complex Variable Method for Boundary Integral Equation of Elasticity. Naukoya, Petersburg.

Martin, P.A., 2000. Perturbed cracks in two dimensions: an integral-equation approach. Int. J. Fract.

Mogilevskaya, S.G., 2000. Complex hypersingular integral equation for the piece-wise homogeneous half-plane with cracks. Int. J. Fract. 102, 177–204.
Muskhelishvili, N.I., 1953. Some Basic Problems of the Mathematical Theory of Elasticity. Noordhoff, Netherlands.
Savruk, M.P., 1981. Two-dimensional Problems of Elasticity for Body with Crack. Naukoya Dumka, Kiev (in Russian).